Nafta-Gaz 2024, no. 5, pp. 288–292, DOI: 10.18668/NG.2024.05.04

Studies of turbulent fluid in a well pump for improving environmental safety

Badania turbulentnego przepływu płynu w pompach głębinowych w celu poprawy bezpieczeństwa środowiskowego

Zamaddin Allakhverdiyev, Latifa Kazimova

Azerbaijan State Oil and Industry University

ABSTRACT: When the plunger moves downwards, the local hydraulic resistance in the injection system causes a hydraulic force from the bottom upwards, which prevents the plunger from falling freely in the cylinder and is the source of the bending of the pump rod column. For this reason, the plunger takes an eccentric position in the cylinder and presses against it, delaying the plunger fall from the head of the balancer of the rocking machine and disturbing coaxial connection of the stock-discharge valve-plunger. These complications lead to increased wear of the plunger-cylinder pair, breakage of the injection valve cell, broken pump rod column, loss of the plunger stroke, etc. It should be noted, however, that in these tests, the flow factor μ is taken as the hydraulic resistance for determining the pressure loss in the valve assembly, and the valve seat cross-section is calculated. When calculating the friction force in the plunger-pressure valve system, the loss of pressure in it is taken to be equal to the loss of pressure of the valve unit. As is known, the downhole pump suction and injection system is a complex system of local resistance, as it consists of different combinations of elements that strongly affect the overall hydraulic resistance of the unit. It is therefore advisable to adopt the local hydraulic resistance coefficient as the hydraulic resistance of the respective unit. The reliability of downhole pumps in general and their individual components is ensured during their design and manufacture and depends on the design features, the quality of manufacturing of components thereof, assembly of the downhole pump in general and their components, as well as a number of other process indicators.

Key words: cylinder, process, plunger-cylinder, downhole pump, rod, injection system, plunger, friction force.

STRESZCZENIE: Podczas ruchu tłoka w dół, na skutek lokalnego oporu hydraulicznego w układzie wtryskowym powstaje siła hydrauliczna działająca od dołu do góry, która uniemożliwia swobodne opadanie tłoka w cylindrze i jest przyczyną wyginania się kolumny tłoczyska pompy. Powoduje to, że tłok przyjmuje mimośrodową pozycję w cylindrze i naciska na niego, opóźniając opadanie tłoka z głowicy wyważarki maszyny wahadłowej i zaburzając współosiowość połączenia tłoka z zaworem wypływu. Komplikacje te prowadzą do zwiększonego zużycia pary tłok-cylinder, uszkodzeń komory zaworu wtryskowego, złamania kolumny tłoczyska pompy, utraty skoku tłoka itp. Należy jednak zauważyć, że w tych testach współczynnik przepływu μ jest przyjmowany jako opór hydrauliczny służący określeniu straty ciśnienia w zespole zaworu, natomiast przekrój gniazda zaworu jest obliczany. Przy obliczaniu siły tarcia w układzie tłok-zawór ciśnieniowy przyjmuje się, że strata ciśnienia jest równa stracie ciśnienia w zespole zaworu. Jak wiadomo, układ ssący i wtryskowy pompy głębinowej jest układem o złożonym oporze lokalnym, ponieważ składa się z różnych kombinacji elementów, które mają znaczący wpływ na całkowity opór hydrauliczny jednostki. Zaleca się zatem przyjęcie współczynnika lokalnego oporu hydraulicznego jako oporu hydraulicznego danej jednostki. Zapewnienie niezawodności pomp wiertniczych ogółem, jak i ich poszczególnych komponentów odbywa się na etapie ich projektowania i produkcji i zależy od cech konstrukcyjnych, jakości wykonania ich komponentów, sposobu wykonania montażu pomp wiertniczych i ich komponentów, a także szeregu innych wskaźników procesowych.

Słowa kluczowe: cylinder, proces, tłok-cylinder, pompa wiertnicza, pręt, układ wtryskowy, tłok, siła tarcia.

Introduction

The plunger takes an eccentric position in the cylinder and presses against it, delaying the plunger fall from the head of the balancer of the rocking machine and disturbing coaxial connection of the stock-discharge valve-plunger (Allakhverdiyev and Ismaylova, 2019). These complications cause increased wear of the plunger-cylinder pair, breakage of the injection valve cell, broken pump rod column, loss of the plunger stroke, etc. A precise determination of the force acting from the bottom up

Corresponding author: L. Kazimova, e-mail: *latifa.ismaylova@gmail.com*

Article contributed to the Editor: 11.12.2023. Approved for publication: 22.04.2024.

will allow the determination of the appropriate weight at the bottom of the pump rod string, ensuring the normal functioning of the well pump. To address several of design issues, it is also advisable to determine the force arising in the downhole pump suction system when the fluid flows through it.

Materials and methods

Consider the general case where the plunger moves downwards and the fluid being displaced rises through the inner cavity of the plunger and the annular space between the cylinder and the plunger. Suppose the plunger velocity is, $un(t)$, and the fluid movement mode is turbulent.

Solution of the problem

The main goal of the research is to achieve the maximum reduction of hydrodynamic friction force.

The research object of the article is the determination of the frictional force generated in the case of non-stationary flow of liquid in the rod well pumps, i.e. in the turbulent regime. When the gap between the plunger and the cylinder is large, the backflow of the fluid increases, leading to lower productivity and increased additional economic costs.

In the process of pumping liquid through a well pump, both its plunger and the sucker rod string directly connected to the plunger, moving down in the upward flow of liquid, experience a hydrodynamic friction force that impedes their movement. This phenomenon is also typical for a well pump when working with hollow rods. Typical tasks regarding this problem are discussed in several works (Dong et al., 2023). Although this problem has been addressed in the referenced works, the back-leakage problem has not been fully resolved. This issue is discussed in detail in the article.

This section discusses in detail the determination of the friction force applied to the inner and outer surfaces of the plunger, as well as to the surface of the sucker rod string, where there is contact with the liquid, with known laws of their motion. As is known, the movement of the plunger and sucker rod string is a function of time. In this case, the corresponding studies were carried out with unsteady motion of fluid flow.

The following expression is used to determine the strength of hydromechanical friction on the surface of the plunger (Onuki Y. and Sugimara J., 2018):

$$T = 2\pi l (r_0\tau_0 + r_1\tau_1) \quad (1)$$

where:

l – length of plunger,

r_0, r_1 – inner and outer radii of plunger, respectively,

τ_0, τ_1 – tangential stress on inner and outer surface of plunger, respectively.

The gap between the cylinder and the plunger shall be divided in two areas at the border of which the velocity profiles shall be closed (Figure 1):

$$u_1 \uparrow_{x_1=a} = u_{2\uparrow_{x=2\delta-a}} \quad (2)$$

u_1 and u_2 are the fluid flow rates in the plunger cavity and annular space, respectively.

Where:

a – the distance from the moving surface to the plane where the profiles are clamped,

δ – the difference between the inner radius of the cylinder and the outer radius of the plunger.

To determine, τ_0, and τ_1, the power speed distribution law can be used (Abdullaev et al., 2006).

As known, the power law of speed distribution has the following form:

$$u = k\left(\frac{\tau g}{\gamma}\right)^{\frac{n+1}{2}}\left(\frac{x}{\vartheta}\right)^n \quad (3)$$

where:

k – coefficient dependent on the Reynolds number,

γ – specific weight of the liquid,

v – kinematic viscosity coefficient of the liquid,

n – degree,

x – distance from the wall towards the center of the current,

τ – shear stress.

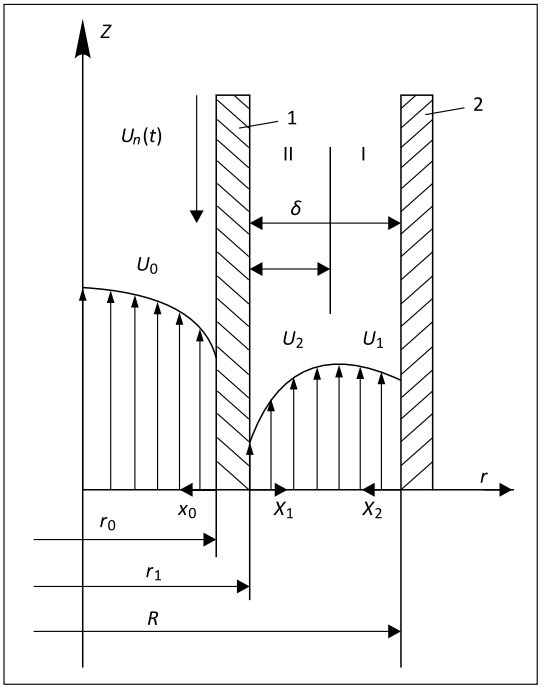

Figure 1. Speed distribution in turbulent fluid flow mode; 1 – plunger, 2 – stationary cylinder

Rysunek 1. Rozkład prędkości w trybie przepływu turbulentnego; 1 – tłok, 2 – nieruchomy cylinder

The natural condition on the pipe axis, as confirmed by experimental data, is:

$$\frac{du}{dx}\uparrow_{x=r_0}=0 \tag{4}$$

This does not satisfy equation (3) because $du/dx\uparrow_{x=r_0}\neq 0$ and $\tau\neq 0$, respectively. Despite this, the condition of (4) is used for such tasks (Kerimov and Allahverdiev, 2002).

Results and discussion

Taking into account the above in order to ensure all the above requirements and requirement (4) of the power law of distribution in the respective areas, the following was chosen:

$$u_0=\left[u_{0\max}+u_n(t)\right]\left[1+\left(1-\frac{x_0}{r_0}\right)^m\right]-u_n(t) \tag{5}$$

$$u_1=\left[u_{\max}+u_n(t)\right]\left[1+\left(1-\frac{x_1}{a}\right)^m\right]-u_n(t) \tag{6}$$

$$U_2=U_{\max}\left[1-\left(1-\frac{x_0}{\delta-a}\right)^m\right] \tag{7}$$

where: u_0 – velocity in the plunger's inner cavity, u_1 – velocity in the first region, u_2 – velocity in the second region, u_0, $u_{\max}$ – maximum velocity in the plunger's inner cavity and in the annular space, respectively (Makovej, 1986).

From (5)–(7), the following can be found:

$$\frac{du_0}{dx_0}=\left[u_{0\max}+u_n(t)\right]\left(1-\frac{x_0}{r_0}\right)^{m-1}\frac{m}{r_0} \tag{8}$$

$$\frac{du_1}{dx_1}=\left[u_{\max}+u_n(t)\right]\left(1-\frac{x_1}{a}\right)^{m-1}\frac{m}{a} \tag{9}$$

$$\frac{du_2}{dx_2}=u_{\max}\left(1-\frac{x}{\delta-a}\right)^{m-1}\frac{m}{\delta-a} \tag{10}$$

As can be seen, the conditions (4) are satisfied in (8) to (10).

Given that tangential stress is determined by the formula:

$$\tau=\frac{du}{dx} \tag{11}$$

for τ_0, τ, τ_1 and τ_2 taking into account (8)–(10), we have:

$$\tau_0=\mu\frac{du_0}{dx_0}\uparrow_{x_0=0}=\mu\left[u_{0\max}+u_n(t)\right]\frac{m}{r_0} \tag{12}$$

$$\tau_1=\mu\frac{du_1}{dx_1}\uparrow_{x_1=0}=\mu\left[u_{\max}+u_n(t)\right]\frac{m}{a} \tag{13}$$

$$\tau_2=\mu\frac{du_2}{dx_2}\uparrow_{x_2=0}=\mu u_{\max}\frac{m}{\delta-a} \tag{14}$$

where μ is the dynamic viscosity of the fluid.

We get from (2) and (3):

$$\frac{\tau_1}{\tau_2}=\frac{\left[u_{0\max}+u_n(t)\right](\delta-a)}{u_{\max}\cdot a} \tag{15}$$

Let us make equations of dynamic equilibrium of the liquid in the inner cavity of the plunger, the annular layer between the moving cylinder and the cylindrical surface on which the tangential stress is zero (area II), and also between the plunger and the stationary cylinder (area I and II):

$$-2\pi r_0 l\tau_0+\pi r_0^2\Delta P=0 \tag{16}$$

$$-2\pi rl\tau_0+\pi\left[R^2-\left(r_1+a\right)^2\right]\Delta P=0 \tag{17}$$

$$-2\pi Rl\tau_2-2\pi r_1 l\tau_1+\pi\left(R^2-r_1^2\right)\Delta P=0 \tag{18}$$

where: R – inner radius of the stationary cylinder, ΔP – pressure difference on the lower and upper sections of the layer in equation (Makovej, 1986).

From (16)–(18), we have:

$$\tau_1=\frac{a(2r_1+a)}{r_0 r_1}\tau_0 \tag{19}$$

$$\tau_2=\frac{R^2-\left(r_1+a\right)^2}{r_0 R}\tau_0 \tag{20}$$

From (19) and (20) we find that:

$$\frac{\tau_1}{\tau_2}=\frac{Ra(2r_1+a)}{r_1\left[R^2-\left(r_1+a\right)^2\right]} \tag{21}$$

From Joint Decision (5) and (21):

$$u_{\max}=u_n(t)\left[\frac{r_1(\delta-a)\left[R^2-\left(r_1+a\right)^2\right]}{a^2R(2r_1+a)-r_1(\delta-a)\left[R^2-\left(r_1+a\right)^2\right]^{-1}}\right] \tag{22}$$

Thus, substituting (2) and (13) in (21), including (2) and (23) as well as values from:

$$u_n(t)=\frac{1}{2}\omega S\sin\omega t \tag{23}$$

$$T=\frac{\pi^2}{30}\mu lm\frac{Rr_1\left[r_0^2+a(2r_1+a)\right]}{a^2R(2r_1+a)-r_1(\delta-a)\left[R^2-(r_1+a)^2\right]}\cdot \cdot(Sn)\sin\omega t \tag{24}$$

To determine the parameter, a, let us make the equation of the fluid flow continuity:

$$\pi(r_1^2-r_0^2)u_n(t)=q_0+q_1+q_2 \tag{25}$$

where: q_0, q_1, q_2 – flow of fluid in the inner cavity of the plunger, the first and second areas of the annular space.

On the other hand, q_0, q_1, q_2 can be defined from the following expressions:

$$q_0 = 2\pi \int_0^{r_0} u_0 x_0 dx_0 \tag{26}$$

$$q_1 = 2\pi \int_0^{a} u_1 (r_1 + x_1) dx_1 \tag{27}$$

$$q_2 = 2\pi \int_0^{\delta - a} u_2 (R - x_2) dx_2 \tag{28}$$

$$q_0 = \pi u_{0\max} r_0^2 - 2\pi [u_{0\max} + u_n(t)] \frac{r_0^2}{(m+1)(m+2)} \tag{29}$$

$$q_1 = \pi u_{\max} (2r_1 + a)a - 2\pi \left[u_{\max} + u_n(t)\right] \frac{a\left[(m+2)r_1 + a\right]}{(m+1)(m+2)} \tag{30}$$

$$q_2 = \pi u_{\max} (\delta - a)(2R - \delta + a)a - 2\pi u_{\max} \cdot \cdot \frac{(\delta - a)[(m+2)R - \delta + a]}{(m+1)(m+2)} \tag{31}$$

By substituting (29)–(31) into (25), we get the expression defining the parameter, a, as follows:

$$\frac{1}{a^2 R(2r_1 + a) - r_1(\delta - a)\left[R^2 - (r_1 + a)^2\right]} \cdot \cdot \left\{ r_1 r_0^4 R - \frac{2r_0^4 r_1 R}{(m+1)(m+2)} + r_1(\delta - a)\left[R^2 - (r_1 + a)^2\right] \cdot \cdot (2r_1 + a)a - \frac{2a^3 R(2r_1 + a)\left[(m+2)r_1 + a\right]}{(m+1)(m+2)} + + r_1(\delta - a)^2\left[R^2 - (r_1 + a)^2\right](2r_1 - \delta + a) - - \frac{2r_1(\delta - a)^2\left[R^2 - (r_1 + a)^2\right]\left[(m+2)R - \delta + a\right]}{(m+1)(m+2)} \right\} - - r_1^2 = 0 \tag{32}$$

Let us consider the choice of degree, m, for our power speed distribution.

Let us determine the average speed in the round tube according to the selected speed distribution:

$$u_{cp} = \frac{2}{r_0^2} \int_{r_0}^{0} urdr = -\frac{2u_{\max}}{r_0^2} \int_{r_0}^{0} \left[1 - \left(1 - \frac{x}{r_0}\right)^m\right](r - x)dx$$

$$\frac{u_{\max}}{u_{cp}} = \frac{m+2}{m} \tag{33}$$

According to (Shin et al., 2019), the ratio of the maximum speed (on the pipe axis) to the mean cross-section of the turbulent tube varies from 1.15 to 1.3 depending on the Reynolds number (Kerimov and Allahverdiev, 2003). The value of n in the power law is within 1/6 n 1/10.

Using formula (33) for a given value, n, having $u_{\max}/u_{cp}$, the following relationship between, m and n is defined, as shown in the Table 1.

Table 1. Relationship between m and n

Tabela 1. Zależność między m i n

n	1/6	1/7	1/8	1/9	1/10
m	7.58	8.93	10.31	11.56	12.82

Thus, with according to m, by equation (32) we find the parameter a, and given it in (24), we can determine the hydromechanical friction force applied to the surface of the plunger. (Bajkov et al., 2003).

Let us consider the individual cases.

Let us assume that the liquid is pushed only through the inner cavity of the plunger. In this case, the friction force will be determined by the formula:

$$T = 2\pi r_0 l \tau_0 \tag{34}$$

From the fluid flow continuity equation, we have:

Taking into account the value, q_0 of (26) in (35), let us determine the maximum speed in the plunger:

$$u_{\max} = u_n(t)\left\{\frac{r_1^2(m+1)(m+2)}{r_0^2(m+1)(m+2) - 2} - 1\right\} \tag{35}$$

(25) and (23):

$$T = \frac{\pi^2}{30} \mu l m \left[\frac{r_1^2(m+1)(m+2)}{r_0^2(m+1)(m+2) - 2}\right](Sn)\sin\omega t \tag{36}$$

Findings: When the downhole pump is operated on hollow rods, given the difference in the internal diameter of the plunger and hollow rod, the friction force in the inner surface of hollow rods should be determined by the formula:

$$T = \frac{\pi^2}{30} l_1 \mu m \left[\frac{(m+1)(m+2)\left(r_1^2 - r_0^2\right) + 2r_\Theta^2}{r_\Theta^2\left[(m+1)(m+2) - 2\right]}\right](Sn)\sin\omega t \tag{37}$$

where:

l_1 – hollow rod length,

r_Θ – inner radius of hollow rods.

Indeed, if $r_\Theta = r_0$, i.e. if there is no difference between the internal radius of the plunger and the hollow rod, the equation (38) is similar to (37).

Thus, when the downhole pump is operated on hollow friction rods in the plunger system, the friction force on the hollow rods will be equal to the sum of the friction force described by the formulas (26) and (27).

Let us assume that when the plunger moves downwards, the liquid is pushed out only through the annular space. In this case $r_0 = 0$ and the friction will be determined by the formula (Reimann et al., 2017):

$$T = 2\pi l r_1 \tau_1 \tag{38}$$

Then the equations (13), (12), (38) are as follows:

$$T = \frac{\pi}{30} l \mu r_1 \frac{m}{a} \cdot \left[\frac{r_1(\delta + a)\left[R^2 - (r_1 + a)^2\right]}{a^2 R(2r_1 + a) - r_1(\delta - a)\left[R^2 - (r_1 + a)^2\right]} + 1 \right] \cdot (Sn) \sin \omega t \quad (39)$$

To define the parameter a, let us write the flow continuity conditions as follows (Saravanan et al., 2016):

$$\pi \dot{r}_1^2 u_n(t) = q_1 + q_2 \quad (40)$$

Then the equations (19) and (20), (30) are as follows:

$$\frac{r_1(\delta - a)\left[R^2 - (r_1 + a)^2\right]}{a^2 R(2r_1 + a) - r_1(\delta - a)\left[R^2 - (r_1 + a)^2\right]} \cdot \{(2r_1 + a)a - \frac{2\left[a + \left((m+2)r_1 + a\right) + (\delta - a)\right]\left[(m+2)R - \delta + a\right]}{(m+1)(m+2)} + (\delta - a)(2R - \delta + a)\} - \frac{2a\left[(m+1)r_1 + a\right]}{(m+1)(m+2)} - r_1^2 = 0 \quad (41)$$

From (41), by defining the parameter a and substituting it into (40), it is possible to determine the friction force applied to the external surface when immersed in the liquid of the cylindrical body, in particular the plunger or pumping rod columns.

Conclusions

Although all downhole pumps of different types have the same size, they exhibit different friction forces at the same pumping parameter. This is due to the fact that the plunger unit comprises various combinations of elements integrated into their design. Consequently, by selecting the appropriate elements, it is possible to reduce the friction in the injection system. At the same time, it is necessary to take into account the hydraulic performance of the elements included in the downhole pump assembly during the completion of any downhole pump assembly with the aim of minimizing the hydraulic resistance.

Thus, by knowing the force exerted on the plunger from the bottom upwards, it is possible to determine the required weight of the pumping rod at the bottom of the pump rod column, which compensates the forces causing the longitudinal bending of the rod during the downward stroke. By reducing the hydraulic resistance coefficient in the "plunger-injection valve" unit, it is possible to reduce the weight of the weighting agent at the bottom of the pump rod column.

References

Abdullaev A.I., Al'bere A., Nadzhafov A.M., 2006. Ocenka inercionnyh nagruzok v novom konstruktivnom reshenii mehanicheskogo privoda shtangovyh nasosov. *Azerbajdzhanskoe Neftjanoe Hozjajstvo*, 9: 46–49.

Allakhverdiyev Z.S., Ismaylova L.A., 2019. Valve unit with a ball deflector. *Onshore and offshore oil and gas well construction, Gubkin University Press*, 9: 46–49.

Bajkov I.R., Somorodov E.A., Solov'ev V.Ja., 2003. Dinamicheskie nagruzki shtangah glubinnyh nasosov i ih vlijanie na bezopasnost' jekspluataciiIzv. Vuzov. *Neft' i Gaz*, 1: 41–45.

Dong X.-W., Li Z.-A., Bian L., Wang M., Jin Z.-B., 2023. Study on chatter suppression in ultrasonic-assisted grinding of thin-walled workpiece of SiCp/Al composites. *Advances in Mechanical Engineering*, 15(6): 85–99. DOI: 10.1177/16878132231177995.

Kerimov O.M., Allahverdiev Z.S., 2002. K voprosu abrazivnogo iznosa soprjazhenija tipa pary plunzher-cilindr. Tezisy dokladov mezhdunarodnoj nauchnoj konferencii. Himija tverdogo tela i sovremennye mikro-i nanotehnologii. *Kislovodsk, Rossija*, 282–283.

Kerimov O.M., Allahverdiev Z.S., 2003. K voprosu razrushenija poverhnostnogo sloja pary plunzher-cilindr SShN. Materialy chetvertij mezhdunarodnoj shkoly-seminara. Sovremennye metody issledovanija i preduprezhdenija korrozionnyh razrushenij. *Udmurtskoj Universitet, Izhevsk*, 1–3.

Makovej N., 1986. Drilling hydraulics. *Nedra, Moskva*, 536.

Onuki Y., Sugimara J., 2018. Experimental Study on Reciprocation Rolling-Sliding Contact with Spin, Toraibarojisuto. *Journal of Japanese Tribologiests*, 63(3): 209–215. DOI: 10.18914/tribologist.17-00018.

Reimann M., Goebel J., dos Santos J.F., 2017. Microstructure and mechanical properties of keyhole repair welds in AA 7075-T651 using refill friction stir spot welding. *Materials & Design*, 132: 283–294. DOI: 10.1016/j.matdes.2017.07.013.

Saravanan V., Rajakumar S., Muruganandam A., 2016. Effect of Friction Stir Welding Process Parameters on Microstructure and Mechanical Properties of Dissimilar AA6061-T6 and AA7075-T6 Aluminum Alloy Joints. *Metallography, Microstructure, and Analysis*, 5(6): 476–485. DOI: 10.1007/s13632-016-0315-8.

Shin J.K., Choi S.R., Ahn S.J., Kim D.W., 2018. Contact ratio analysis of the Rzeppa joint based on full-static modeling. *Mechanism and Machine Theory*, 119: 236–251. DOI: 10.1016/j.mechmachtheory.2017.09.005.

Zamaddin ALLAKHVERDIYEV, Ph.D.
Associate Professor at the Department of Industrial Safety and Labor Protection
Azerbaijan State Oil and Industry University
16/21 Azadliq Ave, AZ1000, Baku, Azerbaijan
E-mail: *sultanelioglu@gmail.com*

Latifa KAZIMOVA, Ph.D.
Department of Industrial Safety and Labor Protection
Azerbaijan State Oil and Industry University
16/21 Azadliq Ave, AZ 1010, Baku, Azerbaijan
E-mail: *latifa.ismaylova@gmail.com*